

1 **Effects of *Enteromyxum* spp. (Myxozoa) infection in the regulation of**
2 **intestinal E-cadherin: turbot against gilthead sea bream**

3 Short title: **Intestinal E-cadherin regulation in enteromyxoses**

4 Paolo Ronza^{a*}; Itziar Estensoro^b; Roberto Bermúdez^{a,c}; Ana Paula Losada^a; Gregorio
5 Pérez-Cordón^{b,d}; Belén G. Pardo^{c,e}; Ariadna Sitjà-Bobadilla^b; M^a Isabel Quiroga^{a,c}

6 ^aDepartamento de Anatomía, Producción Animal y Ciencias Clínicas Veterinarias,
7 Universidade de Santiago de Compostela, Lugo, Spain.

8 ^bFish Pathology Group, Instituto de Acuicultura Torre de la Sal, Castellón, Spain.

9 ^cInstituto de Acuicultura, Universidade de Santiago de Compostela, Santiago de
10 Compostela, Spain

11 ^dCryptosporidium Reference Unit, Public Health Wales, Singleton Hospital, Swansea,
12 UK.

13 ^eDepartamento de Zoología, Genética y Antropología Física, Universidade de Santiago
14 de Compostela, Lugo, Spain.

15 *Corresponding author:

16 Dr. Paolo Ronza

17 Departamento de Anatomía, Producción Animal y Ciencias Clínicas Veterinarias

18 Universidade de Santiago de Compostela - Campus Terra

19 27002 Lugo

20 Phone: (+34) 982822306

21 E-mail: paolo.ronza@usc.es

22 **Acknowledgments**

23 The authors are in debt with Professor Jaume Pérez Sánchez for providing access to the
24 gilthead sea bream transcriptomic database ([http://www.nutrigroup-](http://www.nutrigroup-iats.org/seabreamdb)
25 [iats.org/seabreamdb](http://www.nutrigroup-iats.org/seabreamdb)). The authors thank S. Maceiras, J. Monfort and L. Rodríguez for
26 histological processing, R. del Pozo and L. Insua for technical assistance with the qPCR
27 assays, fish husbandry and samplings and M.C. Piazzon for critical reading of the
28 manuscript. This work has been funded by the Spanish Ministry of Economy and
29 Competitiveness and the European Regional Development Fund (ERDF) through the
30 projects AGL2015-67039-C3-1-R, AGL2015-67039-C3-3-R and AGL-2013-48560-R,
31 and by the Horizon 2020 Framework Programme through ParaFishControl Project
32 (634429). I.E. was contracted under APOSTD/2016/037 grant by the “Generalitat
33 Valenciana” and G.P.-C. under the “Juan de la Cierva” program, granted by the Spanish
34 Ministry of Science and Innovation (JCI-2011-09438).

35 **Data Availability Statement**

36 The authors confirm that the data supporting the findings of this study are available within
37 the article and its supplementary materials.

38 **Abstract**

39 Enteromyxoses are relevant diseases for turbot and gilthead sea bream aquaculture. The
40 myxozoan parasites invade the intestinal mucosa, causing a cachectic syndrome
41 associated to intestinal barrier alteration, nonetheless, their pathological impact is
42 different. Turbot infected by *Enteromyxum scophthalmi* develop more severe intestinal
43 lesions, reaching mortality rates of 100%, whereas in *E. leei*-infected gilthead sea bream,
44 the disease progresses slowly, and mortality rates are lower. The mechanisms underlying
45 the different pathogenesis are still unclear. We studied the distribution and expression
46 changes of E-cadherin, a highly conserved protein of the adherens junctions, in the

47 intestine of both species by immunohistochemistry and quantitative PCR, using the same
48 immunohistochemical protocol and common primers. The regular immunostaining
49 pattern observed in control fish turned into markedly irregular in parasitized turbot,
50 showing an intense immunoreaction at the host-parasite interface. Nevertheless, E-
51 cadherin gene expression was not significantly modulated in this species. On the contrary,
52 no evident changes in the protein distribution were noticed in gilthead sea bream, whereas
53 a significant gene down-regulation occurred in advanced infection. The results contribute
54 to the understanding of the different host-parasite interactions in enteromyxoses. Host
55 and parasite cells appear to establish diverse relationships in these species, which could
56 underlie the different pathological picture.

57 **Keywords:** Enteromyxosis, Myxosporea, cell junctions, intestinal barrier, host-parasite
58 interaction

59 **Introduction**

60 Enteromyxoses caused by the intestinal myxozoan parasites *Enteromyxum scophthalmi*
61 and *E. leei* pose a serious threat for marine aquaculture. These infections show fast
62 spreading in productive units, given the direct fish-to-fish transmission of *Enteromyxum*
63 spp., and provoke relevant economic losses for mortality and worsening of productive
64 performances (Sitjà-Bobadilla & Palenzuela, 2012). The parasitic stages invade the
65 digestive tract and then grow and proliferate in the lining epithelium, causing gut
66 inflammation and impaired absorptive function (Bermúdez et al., 2010; Estensoro et al.,
67 2011; Fleurance et al., 2008; Ronza, Robledo, et al., 2019).

68 *E. scophthalmi* mainly infects turbot (*Scophthalmus maximus*), though Senegalese sole
69 (*Solea senegalensis*) grown in a turbot farm suffering an outbreak were also found to be
70 infected by this myxozoan, although with no obvious disease signs until they were

71 examined (Palenzuela, Redondo, López, & Álvarez-Pellitero, 2007). Turbot is highly
72 susceptible to enteromyxosis, showing serious lesions and high morbidity and mortality
73 rates, to the extent that the disease can affect up to 100% of fish in a farming unit. The
74 infection starts in pyloric caeca or anterior intestine and subsequently spreads along the
75 entire gut (Redondo, Palenzuela, & Álvarez-Pellitero, 2004). Infected fish develop
76 catarrhal enteritis of increasing severity throughout the disease (Bermúdez et al., 2010).
77 On the other hand, *E. leei* affects a wide range of fish species, with different host
78 susceptibility (Sitjà-Bobadilla & Palenzuela, 2012). Sharpsnout sea bream (*Diplodus*
79 *puntazzo*) and tiger puffer (*Takifugu rubripes*) are among the most susceptible species,
80 for which the disease constitutes a limiting factor and threatens the viability of their
81 aquaculture (Rigos & Katharios, 2010). By contrast, enteromyxosis usually causes a
82 subchronic disease in gilthead sea bream (GSB, *Sparus aurata*) with accumulated
83 mortality below 20% (Sitjà-Bobadilla & Palenzuela, 2012). Unlike turbot, the intestinal
84 epithelial integrity is always preserved in GSB, even in the most heavily infected cases
85 (Fleurance et al., 2008). Field and experimental data indicate that the distal part of the
86 intestine is the first and main target site of the parasite in this species (Estensoro,
87 Redondo, Alvarez-Pellitero, & Sitjà-Bobadilla, 2010). In both species, turbot and GSB,
88 the parasitization is associated to a cachectic syndrome characterized by weight loss,
89 anorexia and amyotrophy, and no effective therapeutic options are currently available
90 (Sitjà-Bobadilla & Palenzuela, 2012). The pathogenesis of the diseases involves the loss
91 of the intestinal barrier function, although the mechanisms underlying the differences in
92 the magnitude of the lesions are still unclear (Ronza, Robledo, et al., 2019; Sitjà-Bobadilla
93 & Palenzuela, 2012).

94 E-cadherin is the main protein of the adherens junctions, one of the most important
95 components for epithelial cell-cell junctional integrity. In mammals, its alteration has

96 been reported in a variety of conditions associated to gastrointestinal disorders and has
97 been related to apoptosis, cell shedding and disturbances in secretory cells differentiation
98 (Schneider et al., 2010). In fish, E-cadherin gene expression was modulated in the
99 intestine of Atlantic salmon in response to an experimental dietary treatment affecting
100 intestinal fluid permeability (Hu et al., 2016). It is an evolutionary conserved protein. In
101 particular, the C-terminal region of the protein, corresponding to the cytoplasmic domain,
102 remained quite conserved from Placozoa to human (Hulpiau & van Roy, 2011). Recently,
103 an immunohistochemical technique for the detection of E-cadherin was set up in turbot
104 using an anti-human E-cadherin commercial antibody (Ronza, Villamarín, et al., 2019).
105 In this work, we aimed to advance our knowledge of the pathogenesis of the intestinal
106 barrier dysfunction associated to enteromyxoses, by investigating the changes in the
107 protein distribution and gene expression of E-cadherin in the digestive tract of *E.*
108 *scophthalmi*-infected turbot and *E. leei*-infected GSB. In both species, the
109 immunohistochemical protocol described by Ronza et al. (2019) together with
110 quantitative PCR analysis using common primers was employed.

111 **Materials and Methods**

112 *Experimental design and histopathology*

113 The experimental infection of turbot with *E. scophthalmi* by oral intubation and of GSB
114 with *E. leei* by effluent exposure were previously described (see Estensoro, Calduch-
115 Giner, Kaushik, Pérez-Sánchez, & Sitjà-Bobadilla, 2012; Robledo, Ronza, et al., 2014).
116 Briefly, for turbot, a group of naïve fish received an oral inoculum of infected turbot
117 intestinal scrapings, whereas another group (CTRL) was intubated with PBS. For GSB, a
118 group naïve fish received water effluent from a donor tank holding *E. leei*-infected GSB,
119 whereas another was kept unexposed (CTRL).

120 In both trials, tissue samples were collected at different time points in Bouin's fluid and
121 in RNAlater for histopathological and molecular techniques, respectively. The status of
122 CTRL and experimentally infected fish was assessed by light microscopy on H&E,
123 toluidine blue and Giemsa stained sections. Challenged turbot were classified into three
124 groups (slightly, moderately and severely infected) according to the histopathological
125 grading described by Bermúdez et al. (2010). The pyloric caeca and posterior intestine
126 from 8 CTRL and 8 infected turbot at 24 and 42 days post-inoculation (DPI) were used.
127 In order to increase the uniformity of the samples, infected turbot at 24 DPI were chosen
128 among those graded as moderately infected and turbot at 42 DPI among those graded as
129 severely infected. Challenged GSB were classified into two groups: moderately and
130 severely infected according to a semiquantitative scale described in Picard-Sánchez et al.
131 (2019). Samples used in the study include anterior and posterior intestine of 6 CTRL and
132 10 infected fish at 51, 91 and 133 days post-exposure (DPE). For gene expression, only
133 posterior intestine was used, to have a representative number of fish in each grade.

134 Both infection trials were carried out at the facilities of the Institute of Aquaculture Torre
135 de la Sal (IATS) in accordance with national (Royal Decree RD1201/2005, for the
136 protection of animals used in scientific experiments) and institutional regulations (CSIC,
137 IATS Review Board) and the current European Union legislation on handling
138 experimental animals.

139 *Sequence comparison and primer design*

140 Available E-cadherin nucleotide and aminoacidic sequences from for turbot, human and
141 GSB (GenBank accession numbers MG137250, AB025106.1 and KF861995.1,
142 respectively) were compared using Clustal X 2.0 software, and BLASTN 2.9.0 and
143 BLASTP 2.6.1 online programs (Altschul et al., 1997, 2005; Larkin et al., 2007). Given
144 the protein and gene similarity of E-cadherin between turbot and GSB, common primers

145 were designed, based on the mRNA sequences. After analysis, common sequence regions
146 between turbot and GSB were identified and primers were designed using *Primer Express*
147 Software v2.0 (Applied Biosystems). Primer specificity was checked using NCBI/Primer-
148 BLAST (<http://www.ncbi.nlm.nih.gov/tools/primer-blast/>).

149 *Immunohistochemistry*

150 Paraffin sections (3 μ m thick) from Bouin's fixed tissue samples were dewaxed in xylene
151 and rehydrated through a graded ethanol series. The assays were carried out with a
152 previously developed protocol (Ronza, Villamarín, et al., 2019), using an automated
153 stainer (Dako Autostainer, Dako, Glostrup, Denmark) after the antigen retrieval step, in
154 order to standardize the immunostaining. Briefly, the primary antibody (1:50 working
155 dilution, mouse monoclonal antibody to human E-cadherin, clone NCH-38, M3612,
156 Dako) was incubated during 2 h at room temperature. After 30 min incubation with HRP-
157 labelled secondary antibody, the peroxidase reaction was developed with a
158 diaminobenzidine-positive chromogen (EnVision+ System-HRP kit, K 4011; Dako),
159 achieving the desired signal after 1 min of incubation. The sections were washed three
160 times for 5 min in 0.1 M phosphate buffered saline containing 0.05% Tween-20 between
161 all subsequent steps. After counterstaining with haematoxylin, sections were unloaded by
162 the Autostainer, dehydrated and coverslipped with DePeX mounting medium (Gurr®,
163 BDH Prolabo, VWR International, Ltd. UK). In order to test the specificity of the
164 immunoreaction, positive (human tissue) and negative (replacement of the primary
165 antibody by PBS) controls were included.

166 *Gene expression analysis*

167 Tissue samples preserved in RNAlater were kept at 4°C during 24 h and stored at -20°C
168 until RNA extraction. Total RNA was extracted from tissues of CTRL and challenged
169 fish using TRIZOL Reagent (Life Technologies, Carlsbad, CA, USA) according to the

170 manufacturer's recommendations. RNA quality and quantity were evaluated using a
171 Bioanalyzer (Agilent Technologies) and a NanoDrop® ND-1000 spectrophotometer
172 (NanoDrop® Technologies Inc), respectively. Good quality RNA (RIN > 7.5) was
173 reverse transcribed (1 µg) into cDNA with random primers using AffinityScript Multiple
174 Temperature cDNA Synthesis kit (Agilent Technologies) following the supplier's
175 protocol. The qPCR analysis was carried out in a MX3005P thermocycler (Stratagene)
176 using 2 µl of cDNA per reaction and 300 nM of each primer in a final volume of 20 µl
177 according to the Brilliant III Ultra-Fast SYBR® Green QPCR Master Mix (Agilent
178 Technologies) manufacturer's instructions. The constitutively expressed ribosomal
179 protein S4 (RPS4), proved to be stably expressed in turbot (Robledo, Hernández-Urcera,
180 et al., 2014), was chosen as the house-keeping gene for sample normalisation. Each
181 sample was performed in triplicate for accuracy and error estimation including one
182 reverse-transcription-negative control for each gene. Fluorescence readings at the end of
183 each cycle were used to estimate threshold cycle values (Ct). Values were normalized to
184 RPS4 and fold change at transcript level was determined with the relative quantitative
185 method ($\Delta\Delta C_t$) (Livak & Schmittgen, 2001) using data from CTRL fish as reference
186 values. Prior to quantitative analysis, a standard curve was constructed using six serial
187 dilutions of cDNA (from 1,000 to 0.01 ng) and the efficiency of each primer set was
188 determined. Each sample was analysed for primer-dimer, contamination, or mispriming
189 by inspection of their dissociation curves.

190 *Statistical analysis*

191 The statistical analysis of gene expression in turbot was performed with SPSS Statistics
192 20.0 software (SPSS Inc., Chicago, Illinois, USA). Data were expressed as mean \pm SEM,
193 and significance of differences was determined by Student's *t*-test, after checking that

194 data follow a normal distribution using Shapiro-Wilk test. Results were considered
195 significant at $P < 0.05$.

196 In GSB, data on gene expression was analysed using SPSS 21.0. by one-way analysis of
197 variance (ANOVA) analysis followed by a Student-Newman-Keuls (SNK) post hoc test.
198 A P value < 0.05 was considered statistically significant.

199 **Results**

200 *Histopathology*

201 The most evident differences were noticed at an advanced stage of infection, when both
202 species showed a massive parasitic load in the lining epithelium of the entire intestinal
203 tract (Figure 1A-D). Inflammatory infiltration was observed in the lamina propria-
204 submucosa in both cases, although more severe in turbot. On the other hand, the epithelial
205 alterations were quite different: turbot intestine showed large areas of epithelial sloughing
206 and the characteristic “scalped shape” of the remaining lining epithelium. As well,
207 enterocyte alterations consistent with necrotic and apoptotic changes were often observed
208 (Figure 1A, C).

209 *Sequence comparison and primer design*

210 The alignment performed between turbot and GSB E-cadherin resulted in 80% and 77%
211 identity scores of the nucleotide (Supporting file 1) and aminoacidic sequences,
212 respectively. In addition, the E-cadherin sequences of the two species showed similar
213 results when compared to human: the identity scores of the nucleotide and aminoacidic
214 sequences were 71% and 53%, respectively, in the turbot-human comparison, and 74%
215 and 50% in the case of GSB-human.

216 A set of common primers targeting the conserved regions of E-cadherin was designed
217 (E_CAD-F 5'GGAACGATGTGATGCCAAACT, E_CAD-R

218 CAGCTGCCTTCAGGTTGTCAT) to amplify a fragment of 105 bp in length of the E-
219 cadherin gene in both species (Supporting file 1).

220 *Immunohistochemistry*

221 Homogeneous immunostaining of the lining epithelium located at the cell–cell junction
222 area with a basolateral position was observed in CTRL (healthy) fish of both species
223 (Figure 2A, B). The distribution pattern of E-cadherin in the intestinal mucosa did not
224 substantially change in fish with moderate infection, but a more intense staining was
225 noticed surrounding the parasitic structures in turbot (Figure 2C, D). The severely
226 parasitized specimens of this species showed a clear alteration of the immunostaining,
227 consisting in a disordered and irregular distribution pattern of E-cadherin in the
228 epithelium, with areas of scant immunoreaction interspersed with other of intense
229 staining, particularly at enterocyte-parasite interface (Figure 2E). On the contrary, the
230 distribution pattern did not seem to be particularly affected by the massive presence of
231 parasites in GSB (Figure 2F). Within each species, the immunohistochemical results were
232 analogous between the anterior and posterior part of the intestine (Figure 3A-D).

233 *Gene expression analysis*

234 qPCR assays were developed to analyze the gene expression of E-cadherin in the
235 digestive tract of parasitized turbot and GSB and their respective CTRL. Results showed
236 one clear single peak in each case using the common primers designed, indicating the
237 suitability of the developed method. The transcriptional levels indicated a significant (P
238 < 0.05) down-regulation of E-cadherin in the posterior intestine of severely infected GSB,
239 with a decreasing trend with disease worsening (Figure 4). On the contrary, no significant
240 differences were found between CTRL and infected turbot, neither in anterior nor in the
241 posterior region of the intestine, although both regions showed a trend to up-regulation
242 during moderate infection (Figure 5A, B).

243 Discussion

244 In this work, the immunohistochemical distribution and gene expression of E-cadherin in
245 the intestine of fish parasitized by *Enteromyxum* spp. were analysed. These myxozoan
246 parasites colonize the lining epithelium causing a cachectic syndrome characterized by
247 anorexia and weight loss. Nevertheless, the parasitosis shows a different course
248 depending on the species affected; in particular, turbot shows high mortality rates
249 associated to severe catarrhal enteritis while in GSB the intestinal lesions are milder and
250 mortality rates lower. Understanding the pathophysiology of gut barrier in the
251 pathogenesis of these diseases appears to be key to unravel the mechanisms underlying
252 the different susceptibility.

253 The immunohistochemical results indicate a change in the distribution pattern of E-
254 cadherin in turbot, with loss of homogeneity and enhanced presence at the enterocyte-
255 parasite interface. In other parasitosis leading to intestinal barrier dysfunction, the
256 pathogenesis involves the disassembly of cell-cell junctions and cytoskeleton, including
257 the relocation of junctional proteins (Di Genova & Tonelli, 2016). As well, oxidative
258 stress was demonstrated to induce redistribution of E-cadherin and other junctional
259 proteins, causing an increment in intestinal permeability in mice (Rao, Basuroy, Rao,
260 Karnaky, & Gupta, 2002). In turbot enteromyxosis, evidences of enhanced nitric oxide
261 production and occurrence of oxidative stress have been highlighted (Losada, Bermúdez,
262 Faílde, & Quiroga, 2012; Robledo, Ronza, et al., 2014). The relocation of E-cadherin may
263 play a role in the pathogenesis of the characteristic severe epithelial desquamation
264 observed in this species. It was demonstrated that the loss of E-cadherin from cell-cell
265 junctions is related to anoikis (Fouquet et al., 2004), a form of apoptosis induced by loss
266 of anchorage to the extracellular matrix. The occurrence of anoikis in turbot
267 enteromyxosis was previously hypothesized because of the increasing number of

268 apoptotic enterocytes observed during the infection by histology (Bermúdez et al., 2010)
269 and immunochemistry to active caspase-3 (Losada, Bermúdez, Faílde, de Ocenda, &
270 Quiroga, 2014). Moreover, RNA-seq analysis of the intestine of *E. scopthalmi*-infected
271 turbot also highlighted the up-regulation of different pro-apoptotic genes (Robledo,
272 Ronza, et al., 2014).

273 On the contrary, the presence of *E. leei*, even in the case of severe parasitization, affected
274 to a lesser extent the distribution of E-cadherin in GSB. The labelling pattern did not
275 appear particularly altered compared to CTRL fish and there was no E-cadherin
276 accumulation surrounding the parasite plasmodia. This suggests a different interaction
277 between fish and myxozoan cells in this host-parasite scenario.

278 Once penetrating the host lining epithelium, both *Enteromyxum* species dwell, grow and
279 proliferate in the paracellular space between enterocytes (Cuadrado et al., 2008; Redondo,
280 Quiroga, Palenzuela, Nieto, & Álvarez-Pellitero, 2003). The intricacies of the relationship
281 between host and myxozoan cells and their interaction during the infection are still far to
282 be fully understood. In GSB and turbot enteromyxoses, Redondo & Álvarez-Pellitero
283 (2009, 2010b) demonstrated the involvement of lectin/carbohydrate interactions between
284 host and parasite cells in the mechanisms of adhesion and invasion. These authors
285 suggested that the differences observed between the two fish species could aid to explain
286 the differences in the severity of the related diseases (Redondo & Álvarez-Pellitero,
287 2010a). Nevertheless, the existence, nature and role of cell-cell junctions between these
288 myxozoans and their hosts is an aspect to be elucidated. Myxozoa, as members of the
289 Cnidarian phylum, might theoretically present all ancestral eumetazoan types of cell
290 junctions. However, it is difficult to identify them because they are often atypical or
291 inconspicuous (Gruhl & Okamura, 2015). In addition, it is still unclear how junctions can
292 be formed between cells of different species, given the complexity and specificity of the

293 formation of cell junctions in an organism (Cavey & Lecuit, 2009; Shao et al., 2017).
294 Furthermore, in an infection scenario, the parasite might exploit the host cells' capabilities
295 to form junctions to subvert the defence response or simply to gain purchase of the host,
296 as well as the host may alter the structure of its cell junctions to prevent formation of
297 junctions with parasite cells (Gruhl & Okamura, 2015). Structures resembling gap
298 junctions have been described between plasmodia of *E. scophthalmi* and host intestinal
299 epithelium (Redondo et al., 2003), while close interdigitating membranes of primary cells
300 of *E. leei* with host cells have been observed at TEM (authors' unpublished data). The
301 genomic and transcriptomic characterization of *Enteromyxum* spp. would greatly help to
302 elucidate this aspect, and recently there have been promising progresses on this front
303 (Chang et al., 2015; A. Picard-Sánchez et al., 2017; Shpirer et al., 2014).

304 The scant or even absent development of mature spores of *E. scophthalmi* observed in
305 turbot, both in spontaneous and experimental infections, together with the particular
306 virulence of the parasite in this species has led to the hypothesis that turbot might
307 constitute an accidental host (Bermúdez et al., 2006; Redondo et al., 2004; Redondo,
308 Palenzuela, Riaza, Macías, & Álvarez-Pellitero, 2002). This can suggest an atypical
309 behaviour of *E. scophthalmi* during the infection, and the strong interaction with turbot
310 E-cadherin might also represent a strategy to gain purchase of the host and ensure its
311 survival once the epithelium starts to desquamate. In this sense, the presence of parasitic
312 stages covered by mucosal remnants/detached cells in the intestinal lumen was often
313 reported, and it has been interpreted as a strategy to get protection from external
314 conditions until the invasion of a new host (Bermúdez et al., 2010; Losada et al., 2014;
315 Redondo et al., 2003).

316 The two host-parasite scenarios analysed also showed different results concerning the E-
317 cadherin gene expression. In the present work, a qPCR method has been developed for

318 the amplification of a fragment of E-cadherin gene using common primers for both
319 species. The optimized assay showed good specificity and sensitivity for both fish
320 species. Intestinal E-cadherin down-regulation is usually observed in mammal's diseases
321 characterized by high levels of pro-inflammatory molecules, such is the case of
322 inflammatory bowel disease, where it has been related with the weakening of cell-cell
323 adhesion in the lining epithelium (Arijs et al., 2011; Sanders, 2005). At this purpose, the
324 down-regulation of E-cadherin gene expression found in severely-parasitized GSB, where
325 a strong local immune response has been described (Pérez-Cordón et al., 2014), was the
326 expected result and might underlie the development of intestinal barrier dysfunction in
327 advanced infection. In addition, important changes in goblet cell composition and
328 distribution, intestinal mucin expression and mucus glycoprotein profile have been
329 described in *E. leei*-infected GSB (Estensoro et al., 2013; Estensoro, Redondo, et al.,
330 2012; Pérez-Sánchez et al., 2013), and maturation and positioning of goblet cells was
331 demonstrated to be impaired in mice with the E-cadherin gene inactivated (Schneider et
332 al., 2010). In previous studies in this species, the intestinal gene expression of E-cadherin
333 was also found to be modulated by some dietary interventions. In particular, it was
334 significantly up-regulated in GSB fed a diet low in fish meal and fish oil, and it was
335 restored when sodium butyrate was added (Estensoro et al., 2016). However, no changes
336 were detected when fed with Next Enhance®150 (Pérez-Sánchez et al., 2015) or with
337 olive oil bioactive compounds (Gisbert et al., 2017), and a lower expression was found in
338 the anterior intestine of fish fed DICOSAN or probiotics (Simó-Mirabet et al., 2017).

339 Why the down-regulation of E-cadherin gene expression detected in this study was not
340 accompanied by an observable change in immunostaining in GSB needs to be further
341 analyzed. The analysis of a greater number of time points might help to detect a possible
342 later immunostaining alteration. However, changes in gene expression levels are

343 frequently not reflected at the protein level (Liu, Beyer, & Aebersold, 2016; Vogel &
344 Marcotte, 2012), as well as it is possible that a hypothetical small reduction in E-cadherin
345 synthesis may not be detected by immunohistochemistry. Nevertheless, the distinctive
346 immunolabelling in the parasitized fish of the two species and the different modulation
347 of the gene expression are worthy of further investigation.

348 Remarkably, despite the large body of evidence reporting an exacerbated intestinal
349 immune response in turbot enteromyxosis (Ronza, Robledo, et al., 2019), we did not find
350 a significant modulation of E-cadherin gene expression. A trend of up-regulation was
351 noticed in moderate infection, a stage that, in this species, is characterized by cellular
352 infiltrates in the lining epithelium, consistent with intraepithelial lymphocytes (Bermúdez
353 et al., 2010). An intriguing hypothesis to be further investigated is the possible role of
354 these cells in attempting to preserve the integrity of the intestinal mucosa. Intestinal
355 intraepithelial lymphocytes express junctional molecules, including E-cadherin, and are
356 thought to play a main role in sustaining the epithelial barrier function in mice parasitized
357 by *Eimeria vermiformis* (Inagaki-Ohara et al., 2006).

358 Concluding, this work showed interesting changes of intestinal E-cadherin in both host-
359 parasite scenarios, combining the use of morphopathological and molecular techniques.
360 This is highly recommended in pathogenesis studies to get more exhaustive information,
361 which can also be useful to glimpse the future direction of a research line. The loss of the
362 physiological distribution of E-cadherin and its relocation at the enterocyte-parasite
363 interface in parasitized turbot, whereas no evident changes were noticed in GSB,
364 constitutes a remarkable finding that indicates diverse relationships with the parasite cells
365 according to the host. This might contribute to explain the different host-parasite
366 interactions and disease pathogenicity and deserves further attention. As well, more
367 studies are needed to fully understand the gene expression dynamics of junctional proteins

368 during the diseases. Along with E-cadherin as the main component of the adherens
369 junctions, other proteins constituting the desmosomes and tight junctions (e.g.
370 desmoglein 2, claudins, occludin, zonula occludens) have a relevant role in maintaining
371 the gut barrier integrity, and several works in mammals reported their susceptibility to
372 intestinal inflammation and/or as a target for intestinal parasites (Chelakkot, Ghim, &
373 Ryu, 2018; Di Genova & Tonelli, 2016; Kamekura et al., 2015). To deepen our
374 knowledge of the pathogenesis of barrier dysfunction during enteromyxoses, the
375 exploration of possible perturbances in other junctional complexes should be included,
376 ideally, combining the histopathological observations with transcriptomic and proteomic
377 approaches. Understanding the relative weight of each factor (parasite, host immune
378 response, oxidative stress) in the pathogenesis is crucial towards the design of control and
379 therapeutic measures adapted to the singular fish-parasite model.

380 **References**

- 381 Altschul, S. F., Madden, T. L., Schaffer, A. A., Zhang, J., Zhang, Z., Miller, W., & Lipman, D. J.
382 (1997). Gapped BLAST and PSI-BLAST: a new generation of protein database search
383 programs. *Nucleic Acids Research*, 25, 3389–3402.
384 <https://doi.org/10.1093/nar/25.17.3389>
- 385 Altschul, S. F., Wootton, J. C., Gertz, E. M., Agarwala, R., Morgulis, A., Schaffer, A. A., & Yu, Y. K.
386 (2005). Protein database searches using compositionally adjusted substitution
387 matrices. *FEBS J*, 272, 5101–5109. <https://doi.org/10.1111/j.1742-4658.2005.04945.x>
- 388 Arijs, I., De Hertogh, G., Machiels, K., Van Steen, K., Lemaire, K., Schraenen, A., ... Rutgeerts, P.
389 (2011). Mucosal gene expression of cell adhesion molecules, chemokines, and
390 chemokine receptors in patients with inflammatory bowel disease before and after
391 infliximab treatment. *Am J Gastroenterol*, 106, 748–761.
392 <https://doi.org/10.1038/ajg.2011.27>

393 Bermúdez, R., Losada, A. P., Vázquez, S., Redondo, M. J., Álvarez-Pellitero, P., & Quiroga, M. I.
394 (2010). Light and electron microscopic studies on turbot *Psetta maxima* infected with
395 *Enteromyxum scophthalmi*: Histopathology of turbot enteromyxosis. *Dis Aquat Organ*,
396 89, 209–221. <https://doi.org/10.3354/dao02202>

397 Bermúdez, R., Vigliano, F., Marcaccini, A., Sitjà-Bobadilla, A., Quiroga, M. I., & Nieto, J. M.
398 (2006). Response of Ig-positive cells to *Enteromyxum scophthalmi* (Myxozoa)
399 experimental infection in turbot, *Scophthalmus maximus* (L.): A histopathological and
400 immunohistochemical study. *Fish Shellfish Immunol*, 21, 501–512.
401 <https://doi.org/10.1016/j.fsi.2006.02.006>

402 Cavey, M., & Lecuit, T. (2009). Molecular Bases of Cell–Cell Junctions Stability and Dynamics.
403 *Cold Spring Harbor Perspectives in Biology*, 1(5).
404 <https://doi.org/10.1101/cshperspect.a002998>

405 Chang, E. S., Neuhof, M., Rubinstein, N. D., Diamant, A., Philippe, H., Huchon, D., & Cartwright,
406 P. (2015). Genomic insights into the evolutionary origin of Myxozoa within Cnidaria.
407 *Proc Natl Acad Sci U S A*, 112, 14912–14917.
408 <https://doi.org/10.1073/pnas.1511468112>

409 Chelakkot, C., Ghim, J., & Ryu, S. H. (2018). Mechanisms regulating intestinal barrier integrity
410 and its pathological implications. *Experimental & Molecular Medicine*, 50(8), 1–9.
411 <https://doi.org/10.1038/s12276-018-0126-x>

412 Cuadrado, M., Marques, A., Diamant, A., Sitjà-Bobadilla, A., Palenzuela, O., Alvarez-Pellitero,
413 P., ... Crespo, S. (2008). Ultrastructure of *Enteromyxum leei* (Diamant, Lom, & Dyková,
414 1994) (Myxozoa), an Enteric Parasite Infecting Gilthead Sea Bream (*Sparus aurata*) and
415 Sharpshout Sea Bream (*Diplodus puntazzo*). *Journal of Eukaryotic Microbiology*, 55(3),
416 178–184. <https://doi.org/10.1111/j.1550-7408.2008.00325.x>

417 Di Genova, B. M., & Tonelli, R. R. (2016). Infection Strategies of Intestinal Parasite Pathogens
418 and Host Cell Responses. *Frontiers in Microbiology*, 7.
419 <https://doi.org/10.3389/fmicb.2016.00256>

420 Estensoro, I., Ballester-Lozano, G., Benedito-Palos, L., Grammes, F., Martos-Sitcha, J. A.,
421 Mydland, L.-T., ... Pérez-Sánchez, J. (2016). Dietary Butyrate Helps to Restore the
422 Intestinal Status of a Marine Teleost (*Sparus aurata*) Fed Extreme Diets Low in Fish
423 Meal and Fish Oil. *PLOS ONE*, 11(11), e0166564.
424 <https://doi.org/10.1371/journal.pone.0166564>

425 Estensoro, I., Benedito-Palos, L., Palenzuela, O., Kaushik, S., Sitjà-Bobadilla, A., & Pérez-
426 Sánchez, J. (2011). The nutritional background of the host alters the disease course in a
427 fish–myxosporean system. *Vet Parasitol*, 175, 141–150.
428 <http://dx.doi.org/10.1016/j.vetpar.2010.09.015>

429 Estensoro, I., Calduch-Giner, J. A., Kaushik, S., Pérez-Sánchez, J., & Sitjà-Bobadilla, A. (2012).
430 Modulation of the IgM gene expression and IgM immunoreactive cell distribution by
431 the nutritional background in gilthead sea bream (*Sparus aurata*) challenged with
432 *Enteromyxum leei* (Myxozoa). *Fish Shellfish Immunol*, 33, 401–410.
433 <https://doi.org/10.1016/j.fsi.2012.05.029>

434 Estensoro, I., Jung-Schroers, V., Álvarez-Pellitero, P., Steinhagen, D., & Sitjà-Bobadilla, A.
435 (2013). Effects of *Enteromyxum leei* (Myxozoa) infection on gilthead sea bream (*Sparus*
436 *aurata*) (Teleostei) intestinal mucus: Glycoprotein profile and bacterial adhesion.
437 *Parasitology Research*, 112(2), 567–576. <https://doi.org/10.1007/s00436-012-3168-3>

438 Estensoro, I., Redondo, M. J., Alvarez-Pellitero, P., & Sitjà-Bobadilla, A. (2010). Novel horizontal
439 transmission route for *Enteromyxum leei* (Myxozoa) by anal intubation of gilthead sea
440 bream *Sparus aurata*. *Diseases of Aquatic Organisms*, 92(1), 51–58.
441 <https://doi.org/10.3354/dao02267>

442 Estensoro, I., Redondo, M. J., Salesa, B., Kaushik, S., Pérez-Sánchez, J., & Sitjà-Bobadilla, A.
443 (2012). Effect of nutrition and *Enteromyxum leei* infection on gilthead sea bream
444 *Sparus aurata* intestinal carbohydrate distribution. *Diseases of Aquatic Organisms*,
445 *100*(1), 29–42. <https://doi.org/10.3354/dao02486>

446 Fleurance, R., Sauvegrain, C., Marques, A., Le Breton, A., Guereaud, C., Cherel, Y., & Wyers, M.
447 (2008). Histopathological changes caused by *Enteromyxum leei* infection in farmed sea
448 bream *Sparus aurata*. *Dis Aquat Organ*, *79*, 219–228.
449 <https://doi.org/10.3354/dao01832>

450 Fouquet, S., Lugo-Martinez, V. H., Faussat, A. M., Renaud, F., Cardot, P., Chambaz, J., ... Thenet,
451 S. (2004). Early loss of E-cadherin from cell-cell contacts is involved in the onset of
452 Anoikis in enterocytes. *J Biol Chem*, *279*, 43061–43069.
453 <https://doi.org/10.1074/jbc.M405095200>

454 Gisbert, E., Andree, K. B., Quintela, J. C., Calduch-Giner, J. A., Ipharraguerre, I. R., & Pérez-
455 Sánchez, J. (2017). Olive oil bioactive compounds increase body weight, and improve
456 gut health and integrity in gilthead sea bream (*Sparus aurata*). *British Journal of*
457 *Nutrition*, *117*(3), 351–363. <https://doi.org/10.1017/S0007114517000228>

458 Gruhl, A., & Okamura, B. (2015). Tissue Characteristics and Development in Myxozoa. In B.
459 Okamura, A. Gruhl, & J. L. Bartholomew (Eds.), *Myxozoan Evolution, Ecology and*
460 *Development* (pp. 155–174). https://doi.org/10.1007/978-3-319-14753-6_9

461 Hu, H., Kortner, T. M., Gajardo, K., Chikwati, E., Tinsley, J., & Krogdahl, A. (2016). Intestinal
462 Fluid Permeability in Atlantic Salmon (*Salmo salar* L.) Is Affected by Dietary Protein
463 Source. *PLoS One*, *11*, e0167515. <https://doi.org/10.1371/journal.pone.0167515>

464 Hulpiau, P., & van Roy, F. (2011). New insights into the evolution of metazoan cadherins. *Mol*
465 *Biol Evol*, *28*, 647–657. <https://doi.org/10.1093/molbev/msq233>

466 Inagaki-Ohara, K., Dewi, F. N., Hisaeda, H., Smith, A. L., Jimi, F., Miyahira, M., ... Nawa, Y.
467 (2006). Intestinal Intraepithelial Lymphocytes Sustain the Epithelial Barrier Function

468 against *Eimeria vermiformis* Infection. *Infection and Immunity*, 74(9), 5292–5301.
469 <https://doi.org/10.1128/IAI.02024-05>

470 Kamekura, R., Nava, P., Feng, M., Quiros, M., Nishio, H., Weber, D. A., ... Nusrat, A. (2015).
471 Inflammation-induced desmoglein-2 ectodomain shedding compromises the mucosal
472 barrier. *Mol Biol Cell*, 26, 3165–3177. <https://doi.org/10.1091/mbc.E15-03-0147>

473 Larkin, M. A., Blackshields, G., Brown, N. P., Chenna, R., McGettigan, P. A., McWilliam, H., ...
474 Higgins, D. G. (2007). Clustal W and Clustal X version 2.0. *Bioinformatics*, 23(21), 2947–
475 2948. <https://doi.org/10.1093/bioinformatics/btm404>

476 Liu, Y., Beyer, A., Aebersold, R. (2016). On the Dependency of Cellular Protein Levels on mRNA
477 Abundance. *Cell*, 165(3), 535–550. <https://doi.org/10.1016/j.cell.2016.03.014>

478 Livak, K. J., & Schmittgen, T. D. (2001). Analysis of relative gene expression data using real-time
479 quantitative PCR and the 2^{(-Delta C(T))} Method. *Methods*, 25, 402–408.
480 <https://doi.org/10.1006/meth.2001.1262>

481 Losada, A. P., Bermúdez, R., Faílde, L. D., de Ocenda, M. V. R., & Quiroga, M. I. (2014). Study of
482 the distribution of active caspase-3-positive cells in turbot, *Scophthalmus maximus* (L.),
483 enteromyxosis. *J Fish Dis*, 37, 21–32. <https://doi.org/10.1111/jfd.12029>

484 Losada, A. P., Bermúdez, R., Faílde, L. D., & Quiroga, M. I. (2012). Quantitative and qualitative
485 evaluation of iNOS expression in turbot (*Psetta maxima*) infected with *Enteromyxum*
486 *scophthalmi*. *Fish Shellfish Immunol*, 32, 243–248.
487 <https://doi.org/10.1016/j.fsi.2011.11.007>

488 Palenzuela, O., Redondo, M. J., López, E., & Álvarez-Pellitero, P. (2007). Cultured sole, *Solea*
489 *senegalensis* is susceptible to *Enteromyxum scophthalmi*, the myxozoan parasite
490 causing turbot emaciative enteritis. *Parassitologia*, 49, 73.

491 Pérez-Cordón, G., Estensoro, I., Benedito-Palos, L., Caldach-Giner, J. A., Sitjà-Bobadilla, A., &
492 Pérez-Sánchez, J. (2014). Interleukin gene expression is strongly modulated at the local

493 level in a fish–parasite model. *Fish Shellfish Immunol*, 37, 201–208.
494 <http://dx.doi.org/10.1016/j.fsi.2014.01.022>

495 Pérez-Sánchez, J., Benedito-Palos, L., Estensoro, I., Petropoulos, Y., Calduch-Giner, J. A.,
496 Browdy, C. L., & Sitjà-Bobadilla, A. (2015). Effects of dietary NEXT ENHANCE®150 on
497 growth performance and expression of immune and intestinal integrity related genes
498 in gilthead sea bream (*Sparus aurata* L.). *Fish & Shellfish Immunology*, 44(1), 117–128.
499 <https://doi.org/10.1016/j.fsi.2015.01.039>

500 Pérez-Sánchez, J., Estensoro, I., Redondo, M. J., Calduch-Giner, J. A., Kaushik, S., & Sitjà-
501 Bobadilla, A. (2013). Mucins as Diagnostic and Prognostic Biomarkers in a Fish-Parasite
502 Model: Transcriptional and Functional Analysis. *PLOS ONE*, 8(6), e65457.
503 <https://doi.org/10.1371/journal.pone.0065457>

504 Picard-Sánchez, A., Cañizares, J., Ziarsolo, P., Blanca, J., Montero-Pau, J., Sitjà-Bobadilla, A., &
505 Palenzeula, O. (2017). Filtering and characterization of Enteromyxum spp (Myxozoa)
506 transcriptomes from RNAseq data. *18th International Conference on Diseases of Fish
507 and Shellfish*. Presented at the 18th International Conference on Diseases of Fish and
508 Shellfish, Belfast, UK.

509 Picard-Sánchez, Amparo, Estensoro, I., del Pozo, R., Piazzon, M. C., Palenzuela, O., & Sitjà-
510 Bobadilla, A. (2019). Acquired protective immune response in a fish-myxozoan model
511 encompasses specific antibodies and inflammation resolution. *Fish & Shellfish
512 Immunology*, 90, 349–362. <https://doi.org/10.1016/j.fsi.2019.04.300>

513 Rao, R. K., Basuroy, S., Rao, V. U., Karnaky, K. J., & Gupta, A. (2002). Tyrosine phosphorylation
514 and dissociation of occludin-ZO-1 and E-cadherin-beta-catenin complexes from the
515 cytoskeleton by oxidative stress. *The Biochemical Journal*, 368(Pt 2), 471–481.
516 <https://doi.org/10.1042/BJ20011804>

517 Redondo, M. J., & Álvarez-Pellitero, P. (2009). Lectin histochemical detection of terminal
518 carbohydrate residues in the enteric myxozoan *Enteromyxum leei* parasitizing gilthead

519 seabream *Sparus aurata* (Pisces: Teleostei): A study using light and transmission
520 electron microscopy. *Folia Parasitol (Praha)*, 56, 259–267.

521 Redondo, M. J., & Álvarez-Pellitero, P. (2010a). Carbohydrate patterns in the digestive tract of
522 *Sparus aurata* L. and *Psetta maxima* (L.) (Teleostei) parasitized by *Enteromyxum leei*
523 and *E. scophthalmi* (Myxozoa). *Parasitology International*, 59, 445–453.
524 <https://doi.org/10.1016/j.parint.2010.06.005>

525 Redondo, M. J., & Álvarez-Pellitero, P. (2010b). The effect of lectins on the attachment and
526 invasion of *Enteromyxum scophthalmi* (Myxozoa) in turbot (*Psetta maxima* L.)
527 intestinal epithelium in vitro. *Exp Parasitol*, 126, 577–581.
528 <https://doi.org/10.1016/j.exppara.2010.06.008>

529 Redondo, M. J., Palenzuela, O., & Álvarez-Pellitero, P. (2004). Studies on transmission and life
530 cycle of *Enteromyxum scophthalmi* (Myxozoa), an enteric parasite of turbot
531 *Scophthalmus maximus*. *Folia Parasitol (Praha)*, 51, 188–198.
532 <https://doi.org/10.14411/fp.2004.022>

533 Redondo, M. J., Palenzuela, O., Riaza, A., Macías, A., & Álvarez-Pellitero, P. (2002).
534 Experimental transmission of *Enteromyxum scophthalmi* (Myxozoa), an enteric
535 parasite of turbot *Scophthalmus maximus*. *J Parasitol*, 88, 482–488.
536 [https://doi.org/10.1645/0022-3395\(2002\)088\[0482:ETOESM\]2.0.CO;2](https://doi.org/10.1645/0022-3395(2002)088[0482:ETOESM]2.0.CO;2)

537 Redondo, M. J., Quiroga, M. I., Palenzuela, O., Nieto, J. M., & Álvarez-Pellitero, P. (2003).
538 Ultrastructural studies on the development of *Enteromyxum scophthalmi* (Myxozoa),
539 an enteric parasite of turbot (*Scophthalmus maximus* L.). *Parasitol Res*, 90, 192–202.
540 <https://doi.org/10.1007/s00436-002-0810-5>

541 Rigos, G., & Katharios, P. (2010). Pathological obstacles of newly-introduced fish species in
542 Mediterranean mariculture: A review. *Reviews in Fish Biology and Fisheries*, 20, 47–70.
543 <https://doi.org/10.1007/s11160-009-9120-7>

544 Robledo, D., Hernández-Urcera, J., Cal, R. M., Pardo, B. G., Sánchez, L., Martínez, P., & Vinas, A.
545 (2014). Analysis of qPCR reference gene stability determination methods and a
546 practical approach for efficiency calculation on a turbot (*Scophthalmus maximus*)
547 gonad dataset. *BMC Genomics*, *15*, 648. <https://doi.org/10.1186/1471-2164-15-648>

548 Robledo, D., Ronza, P., Harrison, P. W., Losada, A. P., Bermúdez, R., Pardo, B. G., ... Martínez, P.
549 (2014). RNA-seq analysis reveals significant transcriptome changes in turbot
550 (*Scophthalmus maximus*) suffering severe enteromyxosis. *BMC Genomics*, *15*, 1149.
551 <https://doi.org/10.1186/1471-2164-15-1149>

552 Ronza, P., Robledo, D., Bermúdez, R., Losada, A. P., Pardo, B. G., Martínez, P., & Quiroga, M. I.
553 (2019). Integrating Genomic and Morphological Approaches in Fish Pathology
554 Research: The Case of Turbot (*Scophthalmus maximus*) Enteromyxosis. *Frontiers in*
555 *Genetics*, *10*, 26. <https://doi.org/10.3389/fgene.2019.00026>

556 Ronza, P., Villamarín, A., Méndez, L., Pardo, B. G., Bermúdez, R., & Quiroga, M. I. (2019).
557 Immunohistochemical expression of E-cadherin in different tissues of the teleost fish
558 *Scophthalmus maximus*. *Aquaculture*, *501*, 465–472.
559 <https://doi.org/10.1016/j.aquaculture.2018.12.009>

560 Sanders, D. S. (2005). Mucosal integrity and barrier function in the pathogenesis of early
561 lesions in Crohn's disease. *J Clin Pathol*, *58*, 568–572.
562 <https://doi.org/10.1136/jcp.2004.021840>

563 Schneider, M. R., Dahlhoff, M., Horst, D., Hirschi, B., Trülzsch, K., Müller-Höcker, J., ... Kolligs, F.
564 T. (2010). A Key Role for E-cadherin in Intestinal Homeostasis and Paneth Cell
565 Maturation. *PLoS ONE*, *5*(12). <https://doi.org/10.1371/journal.pone.0014325>

566 Shao, X., Kang, H., Loveless, T., Lee, G. R., Seok, C., Weis, W. I., ... Hardin, J. (2017). Cell-cell
567 adhesion in metazoans relies on evolutionarily conserved features of the α -catenin- β -
568 catenin-binding interface. *The Journal of Biological Chemistry*, *292*(40), 16477–16490.
569 <https://doi.org/10.1074/jbc.M117.795567>

570 Shpirer, E., Chang, E. S., Diamant, A., Rubinstein, N., Cartwright, P., & Huchon, D. (2014).
571 Diversity and evolution of myxozoan minicollagens and nematogalectins. *BMC Evol*
572 *Biol*, 14, 205. <https://doi.org/10.1186/s12862-014-0205-0>

573 Simó-Mirabet, P., Piazzon, M. C., Calduch-Giner, J. A., Ortiz, Á., Puyalto, M., Sitjà-Bobadilla, A.,
574 & Pérez-Sánchez, J. (2017). Sodium salt medium-chain fatty acids and Bacillus-based
575 probiotic strategies to improve growth and intestinal health of gilthead sea bream
576 (*Sparus aurata*). *PeerJ*, 5, e4001–e4001. <https://doi.org/10.7717/peerj.4001>

577 Sitjà-Bobadilla, A., & Palenzuela, O. (2012). *Enteromyxum* Species. In P. T. K. Woo & K.
578 Buchmann (Eds.), *Fish Parasites: Pathobiology and Protection* (pp. 163–176). UK: CABI
579 publishing.

580 Vogel, C., & Marcotte, E. M. (2012). Insights into the regulation of protein abundance from
581 proteomic and transcriptomic analyses. *Nature Reviews. Genetics*, 13(4), 227–232.
582 <https://doi.org/10.1038/nrg3185>

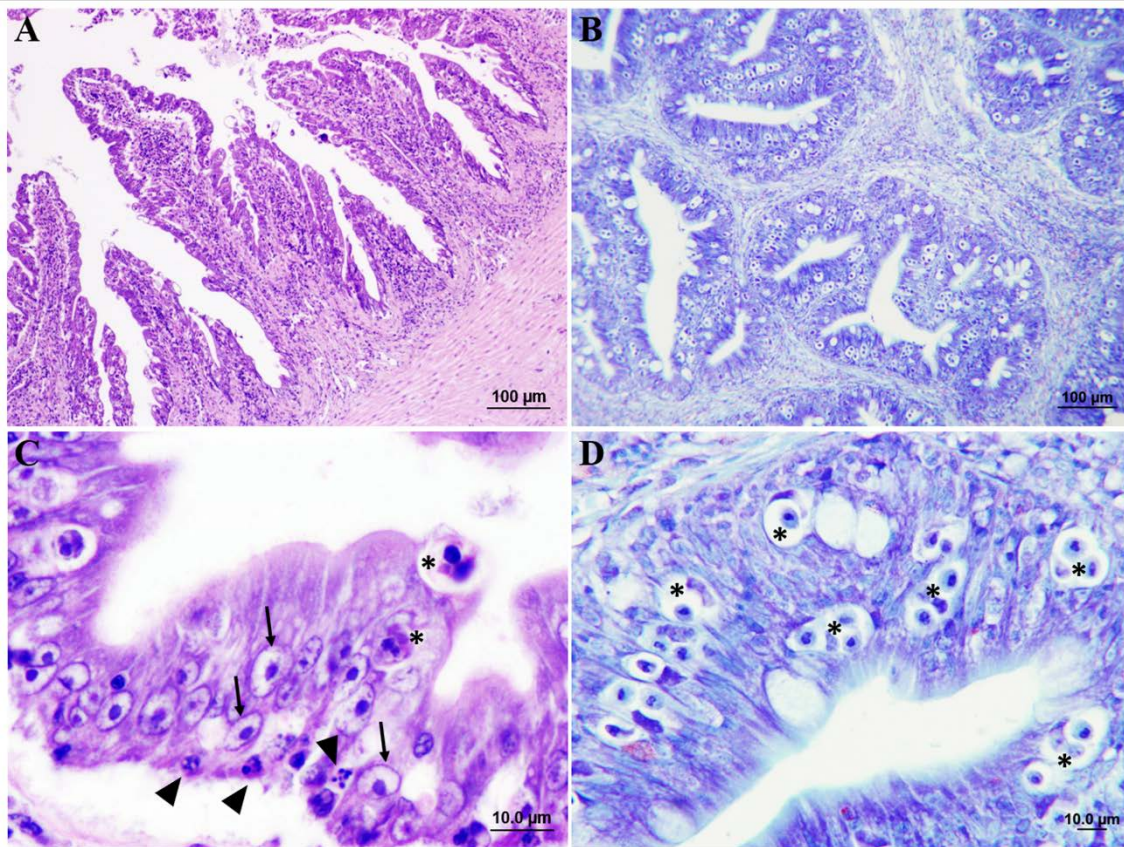
583

584 **Supporting information**

585 (Additional supporting information may be found online in the Supporting Information
586 section)

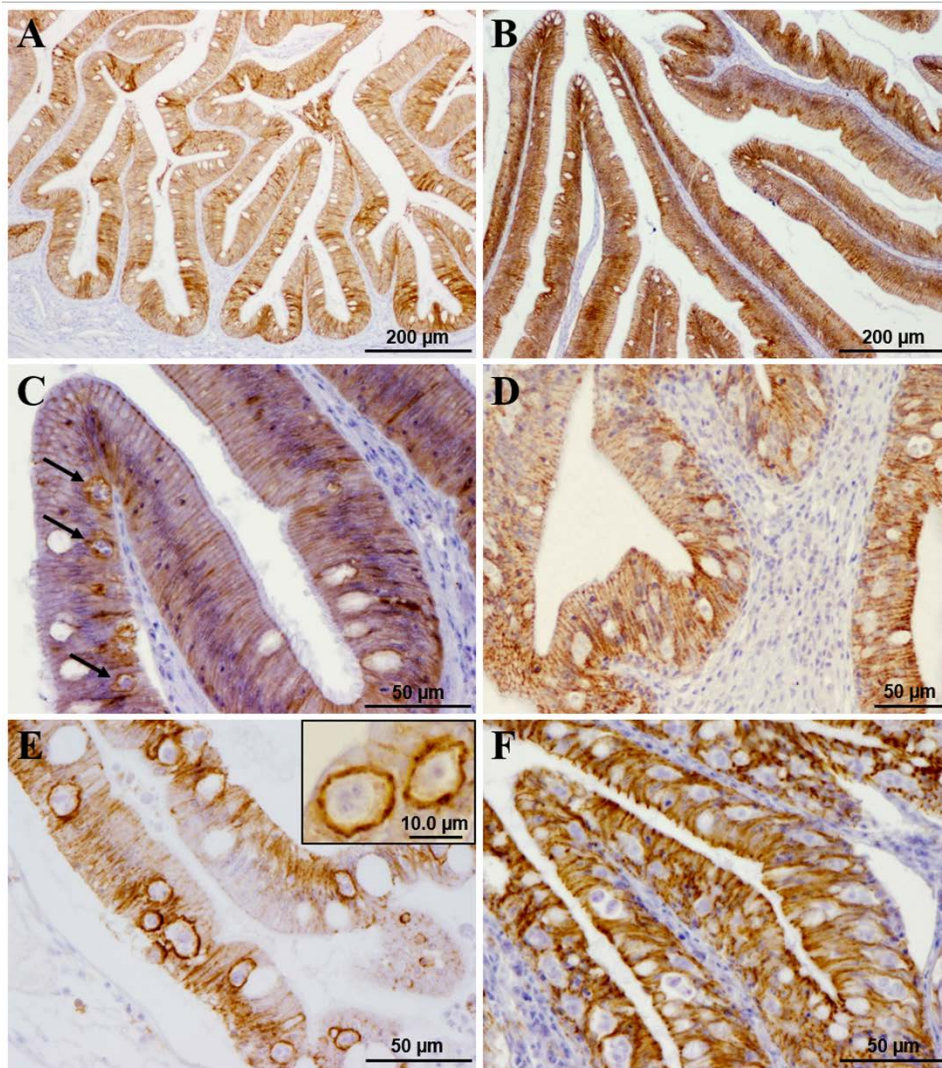
587 **Supporting File 1.** Alignment of E-cadherin nucleotide sequences of turbot
588 (MG137250.1) and gilthead sea bream (KF861995.1). The locations of the primer
589 recognition sites are indicated by arrows.

590



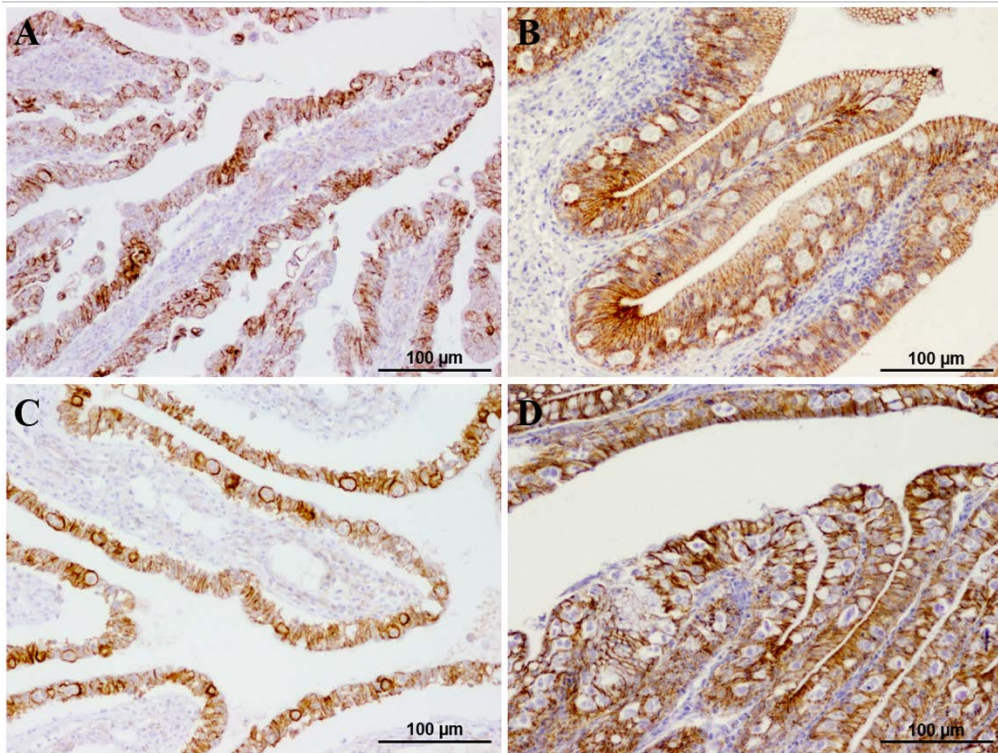
591

592 **Figure 1.** Comparative photomicrographs of turbot pyloric caeca (A, C) and gilthead sea
 593 bream posterior intestine (B, D) with a severe parasitization by *Enteromyxum scophthalmi*
 594 and *E. leei*, respectively. Both species present a high parasite load, but lesions are more
 595 serious in turbot, with a marked inflammatory infiltration in the lamina propria, alteration
 596 of the mucosal architecture and epithelial detachment (A). At higher magnification (C),
 597 apoptotic bodies (arrowheads) and enterocytes with nuclear hypertrophy and central
 598 migration of chromatin (arrows) can be noticed in turbot, associated to the presence of
 599 two parasitic forms (*). By contrast, despite the elevated number of parasites (*), there
 600 are no major alterations in the lining epithelium of gilthead sea bream (D). Haematoxylin
 601 & eosin (A, C) and Giemsa (B, D).



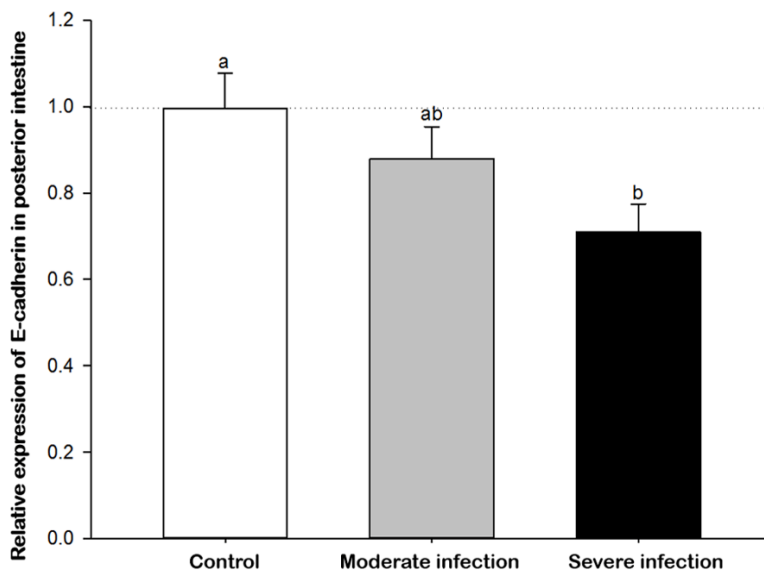
602

603 **Figure 2.** Immunohistochemical detection of E-cadherin in turbot (A, C, E) and gilthead
 604 sea bream (B, D, F) intestine. A, B = Control fish; C, D = *Enteromyxum*-infected fish
 605 with moderate infection; E, F = *Enteromyxum*-infected fish with severe infection. A, B)
 606 E-cadherin immunostaining in control fish showed a regular distribution with
 607 immunolocalization at cell-cell contacts in the intestinal mucosa. Bars = 200 μm . C) In
 608 moderately infected turbot the general distribution pattern of E-cadherin was conserved,
 609 but a more intense immunoreaction was noticed surrounding the parasitic forms (arrows).
 610 Bar = 50 μm . D) No outstanding changes in E-cadherin distribution were noticed in
 611 gilthead sea bream with moderate infection. Bar = 50 μm . E) The immunostaining was
 612 markedly altered in severely parasitized turbot, with areas of scant immunoreaction and
 613 a strong label intensity at the contact areas between host and parasites (see inset). Bar =
 614 50 μm ; Inset bar = 20 μm . F) Even in case of advanced enteromyxosis with a massive
 615 parasite load in the epithelium, E-cadherin immunostaining was not significantly affected
 616 in gilthead sea bream sections. Bar = 50 μm .



617

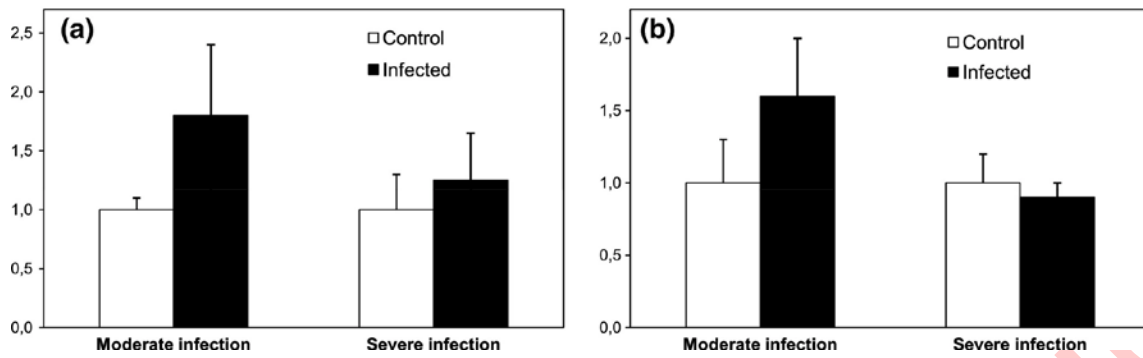
618 **Figure 3.** Comparative photomicrographs of E-cadherin immunostaining in the anterior
 619 (A, B) and posterior (C, D) intestinal regions of severely infected turbot (A, C) and
 620 gilthead sea bream (B, D). Bars = 100 µm.



621

622 **Figure 4.** Mean and standard error of the mean of E-cadherin transcript levels in gilthead
 623 sea bream posterior intestine. Control, moderately and severely *Enteromyxum*-infected
 624 fish were analysed. The transcript levels in control fish were used as reference values
 625 (values > 1 or <1 indicate increase or decrease with respect to the reference). Different
 626 letters indicate statistically significant differences ($P < 0.05$).

627
628



629

630 **Figure 5.** Mean and standard error of the mean of E-cadherin transcript levels in turbot
631 pyloric caeca (A) and posterior intestine (B). Moderately and severely *Enteromyxum*-
632 infected fish at 24 and 42 days post-infection, respectively, were analysed. The transcript
633 levels in the respective control fish groups were used as reference values (values > 1 or
634 <1 indicate increase or decrease with respect to the reference).

635